JACS
JOURNAL OF THE AMERICAN CHEMICAL SOCIETY

Article

pubs.acs.org/JACS

Finding the Right Candidate for the Right Position: A Fast NMR-Assisted Combinatorial Method for Optimizing Nucleic Acids Binders

Ester Jiménez-Moreno,[†] Laura Montalvillo-Jiménez,[†] Andrés G. Santana,[†] Ana M. Gómez,[†] Gonzalo Jiménez-Osés,[‡,§] Francisco Corzana,[‡] Agatha Bastida,[†] Jesús Jiménez-Barbero,[∥,⊥,#] Francisco Javier Cañada,[∥] Irene Gómez-Pinto,[▽] Carlos González,[▽] and Juan Luis Asensio*[,†]

[†]Instituto de Química Orgánica (IQOG-CSIC), Juan de la Cierva 3, 28006 Madrid, Spain

[‡]Departamento de Química y Centro de Investigación en Síntesis Química, Universidad de La Rioja, 26006 Logroño, La Rioja, Spain

[§]Institute of Biocomputation and Physics of Complex Systems (BIFI), University of Zaragoza, BIFI-IQFR (CSIC), 50018 Zaragoza, Spain

[∥]Centro de Investigaciones Biológicas (CIB-CSIC), Ramiro de Maeztu 9, 28040 Madrid, Spain

[⊥]Center for Cooperative Research in Biosciences (CIC-bioGUNE), 48160 Derio, Bizkaia, Spain

[#]Basque Foundation for Science, Ikerbasque, 48013 Bilbao, Bizkaia, Spain

[▽]Instituto de Química-Física Rocasolano (IQFR-CSIC), C/ Serrano 119, 28006 Madrid, Spain

Supporting Information

ABSTRACT: Development of strong and selective binders from promiscuous lead compounds represents one of the most expensive and time-consuming tasks in drug discovery. We herein present a novel fragment-based combinatorial strategy for the optimization of multivalent polyamine scaffolds as DNA/RNA ligands. Our protocol provides a quick access to a large variety of regioisomer libraries that can be tested for selective recognition by combining microdialysis assays with simple isotope labeling and NMR experiments. To illustrate our approach, 20 small libraries comprising 100 novel kanamycin-B derivatives have been prepared and evaluated for selective binding to the ribosomal decoding A-Site sequence. Contrary to the common view of NMR as a low-throughput technique, we demonstrate that our NMR methodology represents a valuable alternative for the detection and quantification of complex mixtures, even integrated by highly similar or structurally related derivatives, a common situation in the context of a lead optimization process. Furthermore, this study provides valuable clues about the structural requirements for selective A-site recognition.

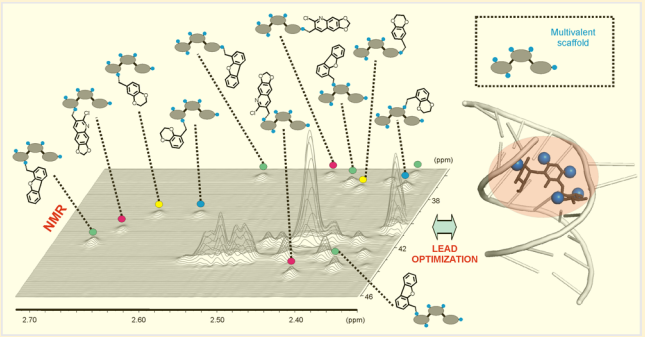

INTRODUCTION

The development of new drugs from bioactive chemical compounds typically involves iterative rounds of synthesis and evaluation, aiming to improve the drug properties and determining the main structure/activity relationships. A conceptually simple fragment-based approach to lead optimization involves decoration of the starting chemical scaffolds with additional fragments. These new functionalities should be carefully selected to increase the shape and chemical complementarity between the drug and the receptor, establishing favorable contacts within the binding pocket (Figure 1a). Unfortunately, in the absence of information provided by experimental structures or computer models, this process is, in most cases, expensive and time-consuming. In particular, the design of improved ligands based on "multivalent" chemical structures, comprising several reactive positions to which fragments could be attached, represents a daunting challenge. In these cases, the number of derivatives to be synthesized and tested through the optimization process expands geometrically with that of the potential anchoring positions in the lead compound. It should be noted that the presence of multiple hydroxyl or amino groups, whose distinct reactivity could be exploited to obtain new derivatives, is a rather widespread structural feature in natural products such as carbohydrates or polyamine RNA/DNA binders (Figures 1a and S1).

Aminoglycosides represent a paradigmatic example of a biologically active multivalent chemical scaffold. These compounds bind to a large variety of RNA/DNA fragments, and, consequently, are promising leads for the development of improved bioactive nucleic acid ligands.[1−4] However, while the presence of multiple positively charged ammonium groups

Received: January 11, 2016
Published: April 28, 2016

DOI: 10.1021/jacs.6b00328
J. Am. Chem. Soc. 2016, 138, 6463−6474

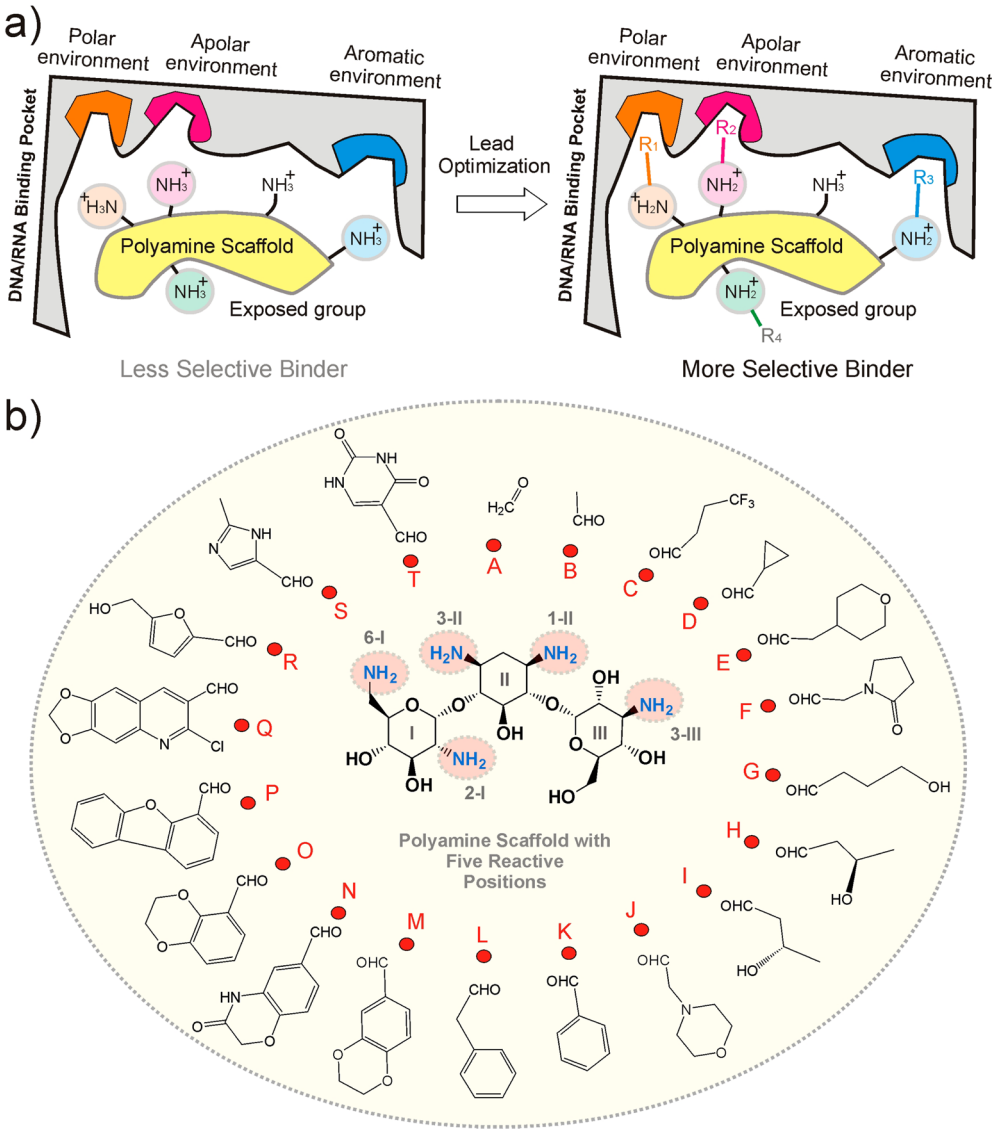

Figure 1. (a) Schematic representation of the fragment-based strategy proposed for the optimization of polyamine binders for selective DNA/RNA recognition (see the main text). (b) Representation of the aldehyde fragments selected for kanamycin-B modification. Reductive amination reactions performed with these molecules rendered 20 small libraries (herein referred as **A**–**T**), each containing five mono-N-substituted kanamycin regio-isomers (see the main text). The numbering employed for the different drug units and reactive positions throughout this manuscript is indicated.

confers a high RNA-binding affinity (usually in the micromolar or submicromolar range), the recognition process exhibits in most cases a low selectivity, which is an expected feature for electrostatically driven associations. For example, kanamycin-B binding affinity for RNA fragments containing the A-site sequence (a natural target) has been shown to be only 1.9- to 2.2-fold larger than that exhibited for the enantiomeric oligo- or mutated versions of the natural receptor (Figure S2).[5,6]

Since the limited capacity to discriminate among different nucleic acid sequences/structures constitutes a general problem for polyamine DNA/RNA binders,[7] the design of new strategies to tackle this problem will have a significant impact in the field of nucleic-acid recognition, and also in drug discovery.

Combinatorial and dynamic combinatorial chemistry[8,9] represent important and efficient approaches for the identification and optimization of lead compounds. Our group has been previously involved in the design of dynamic combinatorial strategies within the aminoglycoside field.[10] We herein present a completely novel fragment-based methodology for the development of selective DNA/RNA ligands from promiscuous polyamine binders, such as aminoglycosides. Our protocol provides a straightforward access to a large variety of small regioisomer libraries. Moreover, the obtained ligand mixtures can be evaluated, in a second step, as selective RNA-binders, employing a simple strategy that combines microdialysis, isotopic labeling and NMR experiments. Overall, this method constitutes a fast, simple and highly parallelizable approach. To validate and analyze the scope and limitations of this methodology, 20 kanamycin-B libraries comprising 100 new derivatives (five per library) have been prepared and tested for selective binding to the ribosomal A-Site RNA. Our results provide important clues about the structural requirements for selective A-site recognition. Most importantly, from a methodological perspective, this work demonstrates that NMR provides a sensitive and simple mean to analyze mixtures of highly similar regio-isomer derivatives.

DOI: 10.1021/jacs.6b00328
J. Am. Chem. Soc. 2016, 138, 6463–6474

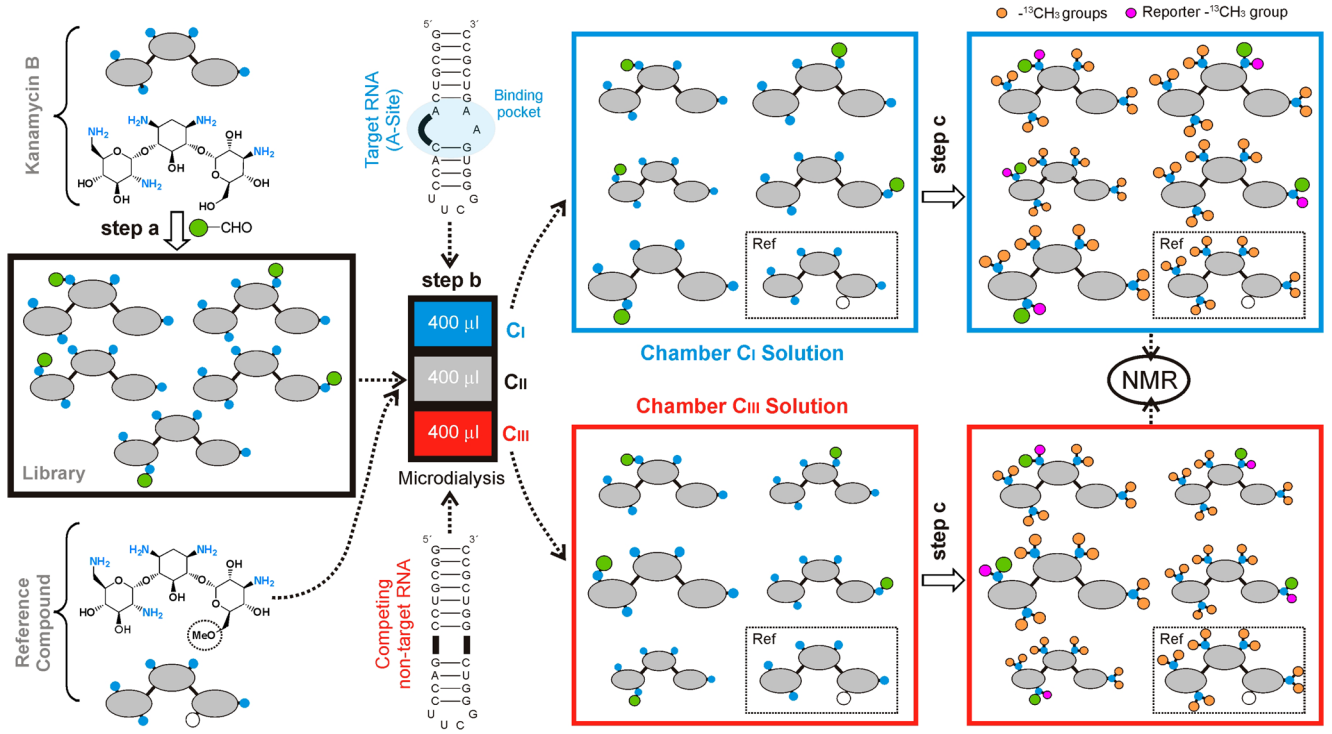

Figure 2. Schematic representation of the experimental protocol designed for the optimization of polyamine binders for selective DNA/RNA recognition (Steps **a** and **b**; see the main text).

RESULTS

Description of the Lead Optimization Strategy. To illustrate our strategy, kanamycin-B (Figure 1b) was selected as model lead compound. This natural product carries five amino functions whose distinct reactivity can be exploited to generate a large variety of non-natural derivatives (Figure 1a,b). Indeed, conventional reductive amination reactions offer a direct mean to attach alternative modulating fragments to the aminoglycoside scaffold. *In simple terms, the optimization process implies finding the right substituent for the right position*; in other words, identifying, for every drug reactive position, a substituent whose chemical properties matches those of its local environment within the receptor binding pocket (Figure 1a). To this end, we selected 20 simple aldehyde molecules spanning a diversity of chemical properties. Our choice included compounds with aldehyde moieties attached to polar, apolar, aliphatic, aromatic, neutral and charged chemical fragments (Figure 1b), some of them relatively common in DNA/RNA binders (see the Supporting Information for a more detailed description of the rationale behind this selection). It should be noted that, given the pentavalent character of kanamycin-B, a systematic investigation of the influence exerted by each of these fragments on the ligand binding properties, by conventional medicinal chemistry approaches, would imply the synthesis, purification and evaluation of 100 new aminoglycoside derivatives, which is an inevitably expensive and time-consuming task. On the contrary, the methodology described herein offers a much faster avenue to lead optimization. Our basic strategy is outlined in Figures 2 and 3 and comprises three distinct steps (referred as **a**–**c**):

*Step **a**: One-Pot Preparation of Kanamycin-B Libraries.* Small regioisomer libraries were generated via reductive amination, employing kanamycin-B and the aldehydes shown in Figure 1b. In a general experiment, a solution of the aminoglycoside (1 mL, 50–70 mM) in buffered water was treated with a substoichiometric amount of an aldehyde (5–10 mM) and sodium cyanoborohydride to generate five monosubstituted derivatives that can be easily purified, as a mixture, by flash chromatography (see the Experimental Section). In this simple way, we obtained 20 different cocktails (one per aldehyde), each containing a distinct distribution of the five possible regioisomers (Libraries **A**–**T** in Figure 1). These distributions were found to be dependent on the chemical nature of the aldehyde and on the accessibility of the different reactive ammonium positions of kanamycin-B. Interestingly, they exhibited an even more significant sensitivity to other experimental parameters such the pK_a of the amino groups and the pH of the reaction buffer, which allowed a certain control on the composition of the mixtures. Consequently, selected libraries were generated under different pH conditions to render alternative regioisomer populations (see below).

*Step **b**: Evaluation of the Libraries for Selective RNA Recognition.* It is important to note that the derivatives considered in this study are polycationic molecules, with a net charge equal or even larger than that of natural kanamycin, which, most likely, should determine a significant nucleic acids binding activity for all of them. However, from a medicinal chemistry perspective, affinity by itself is of little value, being selectivity an essential requirement for DNA/RNA ligands of potential therapeutic use. Taking this consideration into account, we tested the RNA binding properties of the different cocktails using a simple microdialysis protocol specifically designed to reveal the possible changes in the drug selectivity promoted by the attached chemical fragments. To this aim, we employed a device equipped with three chambers (herein referred as C_I–C_{III}; see Figure 2) separated by a 5 kDa cutoff membrane, which allows the free diffusion of the ligands. Thus,

DOI: 10.1021/jacs.6b00328
J. Am. Chem. Soc. 2016, 138, 6463–6474

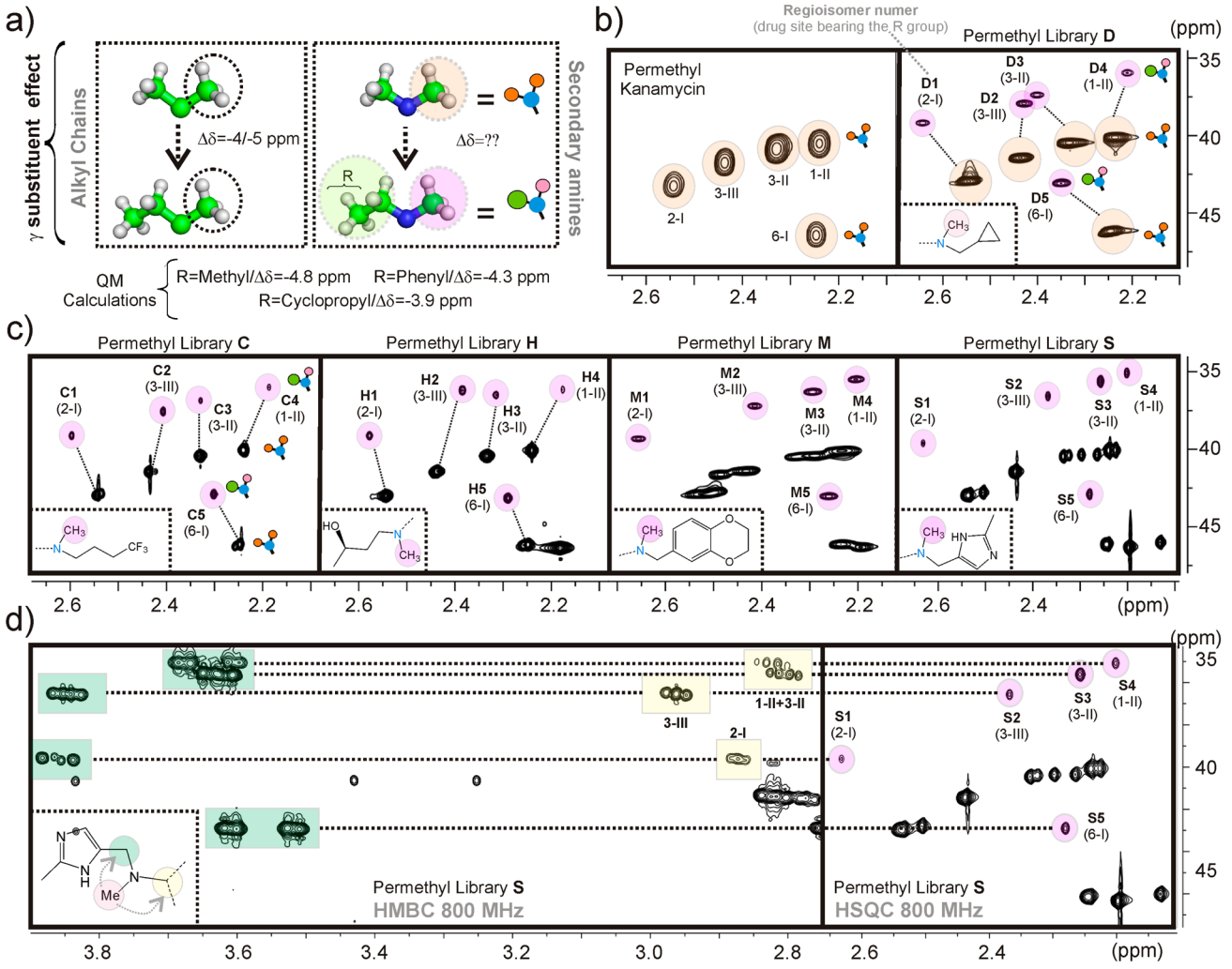

Figure 3. (a) Effect exerted by γ-substitution on the carbon chemical shifts in alkyl chains (left panel).[13] The analogous effects for secondary amines (right panel) have been estimated through quantum mechanics calculations, considering different R substituents (see the Experimental Section). (b) HSQC spectra acquired for permethylated kanamycin (left) and library **D** (right). Reporter methyl cross-peaks ($N^{13}MeR$) for the five regioisomers present in **D** (named as **D1**−**D5**), and $N^{13}Me_2$ signals (present in both data sets) are highlighted with pink and orange circles, respectively. Kanamycin positions bearing the ethyl moiety in regioisomers **D1**−**D5** are indicated in brackets. (c) HSQC spectra acquired for permethylated libraries **C**, **H**, **M**, and **S**. (d) HSQC (right) and HMBC (left) spectra measured for permethylated library **S**. Reporter ^{13}Me groups for the different derivatives (pink circles) exhibit clear 3-bond connections with both the kanamycin core (yellow squares) and the amino substituent R (green squares).

400 μL of a given kanamycin-B library (one library at a time unless explicitly stated) was placed in the central compartment (C_{II}) and dialyzed simultaneously against two separate 400 μL RNA solutions: one containing the target receptor (in chamber C_I) and the other one a competing duplex that lacks the aminoglycoside binding pocket (in chamber C_{III}). Kanamycin binding to this nontarget RNA was taken as representative of a purely electrostatic, unspecific association mode. For comparison purposes, a common reference ligand (herein referred as **Ref**, see below) was externally added to all tested aminoglycoside solutions (Figure 2).

After equilibration, the different mixture components are distributed among the three chambers (C_I−C_{III}), reaching distinct equilibrium concentrations (quantified as described below. Step **c**). Microdialysis experimental parameters were carefully adjusted, paying special attention to the total aminoglycoside concentration (typically in the 80−130 μM range), which was kept in the same range of that of the RNA fragments (100 μM). According to theoretical simulations (see the Experimental Section and Figures S3−S7), under these conditions, the ratio between equilibrium concentrations in chambers C_I and C_{III} for a given library component (herein referred to as "selectivity parameter" and denoted by **Sel**) describes its preference for the RNA receptor with respect to the nonspecific competitor. Similarly, the corresponding ratios for chambers C_I/C_{II} (referred to as affinity parameter or **Af**) can be taken as an indication of the net binding strengths for the different derivatives tested (this was estimated only for selected mixtures). Both parameters were normalized with respect to those measured for the reference compound (**Ref**), present in all the microdialysis assays (normalized values are denoted as $\mathbf{Sel}_N$ and $\mathbf{Af}_N$).

All experiments described throughout the manuscript were carried out employing the prokaryotic ribosomal A-site,[1,2a] a medically relevant target commonly associated with the antibiotic activity of aminoglycosides, as RNA receptor (Figure 2).[11] According to microcalorimetry experiments, kanamycin-B binds to the RNA internal loop with $K_b = 7.6 \times 10^5$ M^{-1} under

DOI: 10.1021/jacs.6b00328
J. Am. Chem. Soc. 2016, 138, 6463−6474

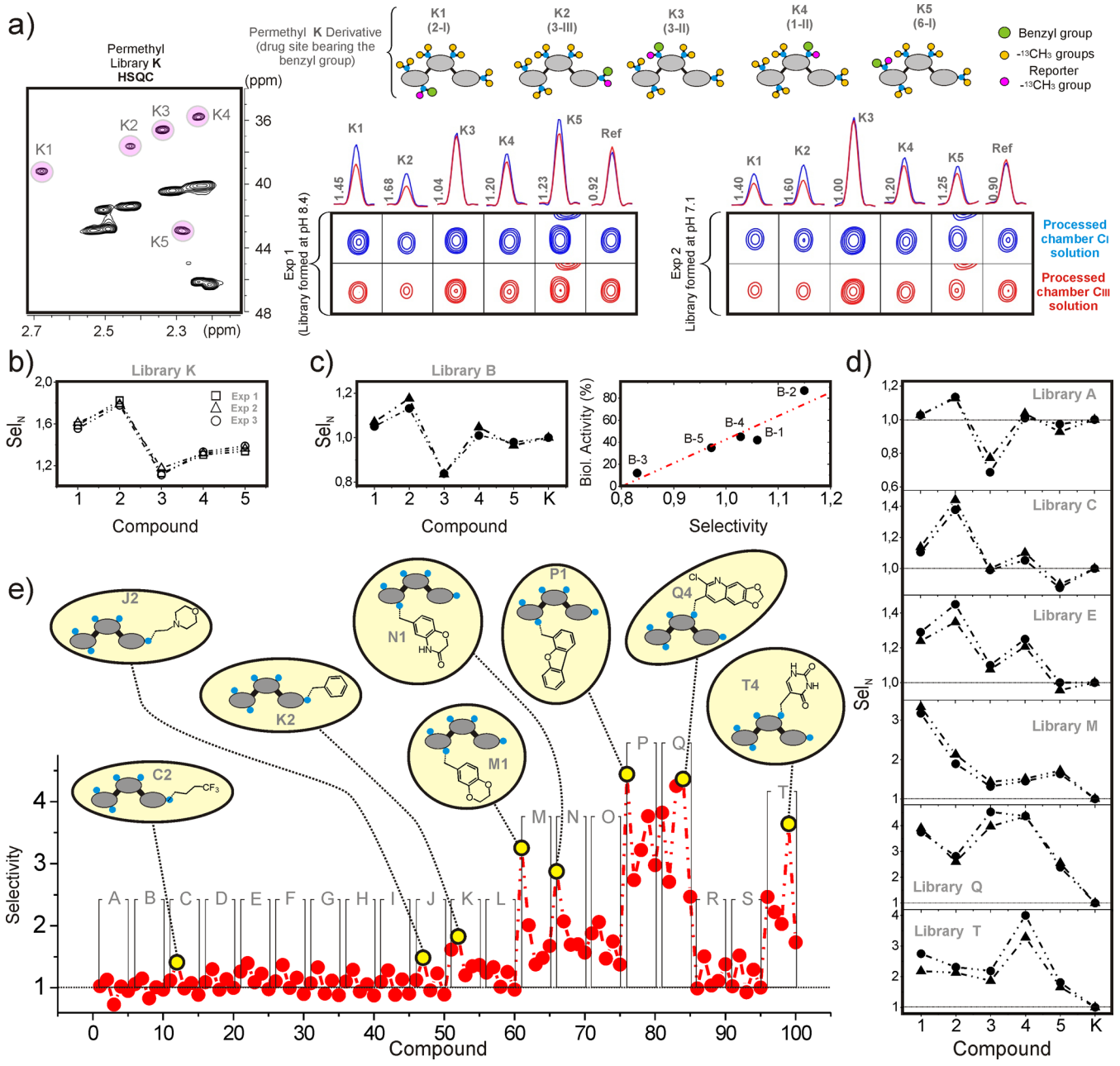

Figure 4. (a) Left: Sample HSQC spectra acquired for permethylated Library **K**. Key reporter methyl signals are highlighted with a pink circle. Right: Assays performed with library **K** generated at pH 8.4 and 7.1 (exp 1 and 3, respectively). Equilibrated microdialysis solutions, present in chambers C_I and C_{III}, were processed according to our protocol and analyzed through HSQC experiments. Reporter methyl signals in the corresponding data sets (shown in blue and red) were integrated to derive a selectivity parameter for every kanamycin derivative (also shown in gray). (b) Selectivity profiles measured for library **K** employing three different mixtures with alternative regioisomer distributions (generated at pH values 8.4, 7.8, and 7.1. Experiments 1−3, respectively). (c) Selectivity profiles measured for library **B** from duplicated microdialysis experiments. The obtained values showed a good correlation with the antibiotic activities described for the different mono-*N*-ethyl kanamycin derivatives (expresses as % with respect to that of kanamycin-B).[15] (d) Selectivity profiles measured for selected libraries from duplicated microdialysis experiments. (e) Selectivity profiles measured for the entire data set (formed by 20 libraries and 100 kanamycin derivatives). Some of representative compounds are highlighted in yellow.

the microdialysis buffer conditions (see Figure S8). As the competing fragment, we used a mutated version of the ribosomal A-site lacking the internal loop-binding pocket (Figure 2).

Finally, a synthetic kanamycin-B derivative with a ^{13}C-labeled OMe group (at position 6-I) was selected as the reference compound (**Ref**, Figure 2). This ligand, synthesized by conventional methods, has been previously described (in its unlabeled form) and is known to exhibit a reasonable antibiotic activity.[12]

*Step **c**: NMR-Based Analysis and Quantification of the Equilibrated Microdialysis Solutions.* The next step involves the deconvolution of the equilibrated microdialysis solutions. These are formed by a low concentration (usually in the 2−25 μM range) of highly similar regioisomers, lacking, in many cases, any chromophoric function. As a consequence, their

DOI: 10.1021/jacs.6b00328
J. Am. Chem. Soc. 2016, 138, 6463−6474

analysis by conventional methods, such as HPLC chromatography, is far from trivial and a different approach has to be envisaged.

Our general strategy is based on getting a simple diagnostic of the solutions by using the NMR-based strategy outlined in Figure 2 (step **c**). First, bound ligands were released by digesting the RNA fragments with RNAase-B. Next, a NMR-sensitive reporter was introduced in the aminoglycoside scaffolds. To this aim, the different solutions were treated with an excess of ^{13}C-labeled formaldeyde and sodium cyanoborohydride to yield a mixture of ^{13}C-enriched permethylated kanamycin derivatives, readily detectable by conventional heteronuclear NMR experiments. It should be noted that, after derivatization, each kanamycin regioisomer incorporates four -N^{13}Me$_2$ moieties and a single -N^{13}**Me**R group (see Figure 2). *This latter function is unique for every single derivative and, provided that it yields a nonoverlapping NMR peak, can be employed as a probe for detection and quantification purposes.*

HSQC experiments acquired with permethylated kanamycin libraries demonstrate that the ^{13}C-labeled methyl groups present at the N^{13}**Me**R fragments produce well-resolved signals that appear, in all cases, 4−5 ppm upfield shifted in the carbon dimensions with respect of those at the N^{13}Me$_2$ moieties (Figures 3 and S9−S12). The origin of this peculiar behavior is that ^{13}C-labeled methyl groups in N^{13}**Me**R fragments have an extra γ-substituent located in the differentiating group R (Figure 3a), which has a remarkable influence on their carbon chemical shifts. In fact, this "γ-effect" was described more than 40 years ago for alkyl chains,[13] and according to our data, is also operative for tertiary amine fragments (a conclusion supported by quantum mechanics calculations. See Figure 3a). As an example, Figure 3b (see also Figure S9) shows the standard HSQC experiments acquired for pure kanamycin-B (left) and library **D** (right) upon reaction with ^{13}C-labeled formaldehyde. It can be observed that the former spectrum presents five well-resolved peaks, corresponding to the different −N^{13}Me$_2$ groups present in the modified aminoglycoside (the assignment is indicated).[10] Interestingly, the permethylated library **D** (formed by five pseudotrisaccharide derivatives) yields an HSQC spectrum of similar complexity. Indeed, this data set displays just five additional methyl cross-peaks (one per -N^{13}**Me**R fragment) upfield shifted by the "γ-effect". Other kanamycin mixtures, especially those bearing aromatic substituents (see Figures 3c and S10 and S11) produced more complex spectra upon methylation. However, in all cases, -N^{13}**Me**R markers can be easily identified and assigned through HMBC spectra. These experiments allow establishing unambiguous 3-bond connections between the methyl groups and both the kanamycin core and the amino substituent R (Figures 3d and S12). Finally, the reference compound (**Ref**) incorporates a distinct O^{13}CH$_3$ appearing in a different spectral region.

In summary, despite the chemical complexity of the microdialysis mixtures (formed by six different pseudotrisaccharide derivatives), they can be processed (Figure 2) to yield relatively simple HSQC spectra with resolved cross peaks for every single component of the mixture.

As a final point, for library **A**, we employed a simplified version of the general protocol. In contrast with mixtures **B**−**T**, this particular cocktail was generated directly in its ^{13}C-labeled form employing ^{13}C-formaldehyde (in step **a**), and therefore, no permethylation was required prior to the NMR analysis (in step **c**. See the Experimental Section).

Proof of Principle: Optimizing Kanamycin Scaffold for Selective A-Site Recognition. To demonstrate the validity of our approach, mixtures **A**−**T** (see Figure 1) were tested for selective binding to the medically relevant A-site RNA (Figures 2 and 4). For library **K**, microdialysis experiments were repeated employing cocktails with three different regioisomer distributions. The obtained results were found to be independent of the mixture stoichiometry (Figures 4a,b and S13). The selectivity profiles derived for particular mixtures are shown in Figure 4b−d. Figure 4e shows the complete profile determined for the entire data set (100 derivatives) from these experiments (see also Figures S13−S15).

Several trends are apparent from this data:

(a) First, the alkyl fragments present in libraries **A**−**D** (see Figures 4c,d and S15) seem to exert a similar influence on the binding process. More specifically, kanamycin substitution at position 3-III (herein referred as regioisomers 2) is in all cases favored, while functionalization at positions 3-II (regioisomers 3) and 6-I (regioisomers 5) tends to be highly disruptive for selective association. It should be noted that this result is fully consistent with the structural information available from crystallographic aminoglycoside/A-site complexes[2a,14] and also with the most frequent modifications of the kanamycin scaffold found in nature.[1] In particular, X-ray diffraction analysis has shown that kanamycin positions 3-II and 6-I (modified in regioisomers 3 and 5, respectively) are involved in extensive hydrogen-bonding interactions with the receptor. Consequently, these positions are totally occluded by the RNA, explaining the negative influence found for alkyl chains at these sites. Moreover, position 3-III (whose modification seems specially favored in terms of selectivity) appears functionalized with alkyl fragments in a significant number of structurally related aminoglycosides.[1] Interestingly, the antibiotic activities reported for the five mono-*N*-ethyl kanamycin regioisomers (compounds **B1**−**B5**)[15] show a good correlation with the selectivity profile deduced for library **B** (see Figure 4c).

(b) A similar trend is evidenced for other non-alkyl fragments (as those present in libraries **E** or **F**), which underlines the special character of kanamycin position 3-III as a preferred modification site for selectivity optimization. However, this behavior is not totally general and the optimal drug modification site depends, to some extent, on the precise nature of the incorporated substituent (Figure 4d,e). Thus, preferred kanamycin position for fragments **M** or **N** is 2-I (regioisomer 1). In contrast, fragment **T** is specially favored at position 1-II (regioisomer 4) and fragment **Q** at positions 3-II or 1-II (regioisomers 3 and 4, respectively). Overall, the tested libraries exhibit a large variety of selectivity profiles from which a single observation seems to be truly general; position 6-I is, in all cases, one of the most disfavored sites for chemical modification (especially with large aldehydes).

(c) The size of the fragment incorporated to the aminoglicoside scaffold is an important selectivity-determining factor. Overall, it can be observed that larger substituents tend to increase the ligand selectivity for the A-site RNA receptor. Accordingly, a significant fraction of the analyzed derivatives exhibits higher selectivities than the smaller reference compound **Ref** (Figure 4e). This behavior can be rationalized by considering that aminoglicosides bind to the RNA major groove,[1,2a,4,14] which is significantly enlarged in the A-site receptor by an internal loop motif. Our data strongly suggests that the binding of bulkier ligands to the narrower major groove of the (competing) canonical duplex is hindered, and

DOI: 10.1021/jacs.6b00328
J. Am. Chem. Soc. 2016, 138, 6463−6474

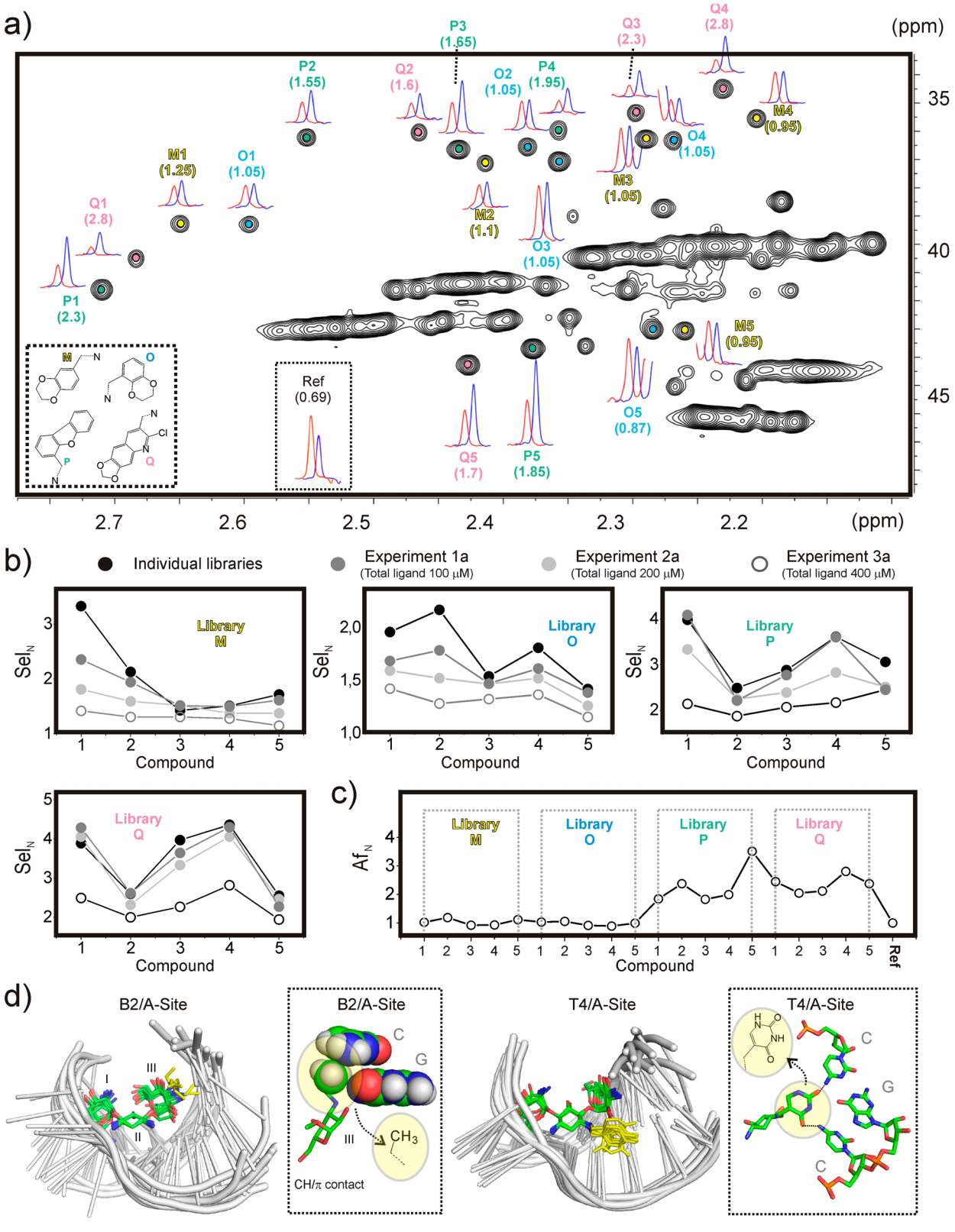

Figure 5. Microdialysis assays performed with mixtures **M** + **O** + **P** + **Q** (experiments 1a−3a. See the main text). (a) HSQC spectrum acquired with a processed A-site containing solution (from microdialysis chamber C_I in experiment 2a). Cross sections for the key cross peaks in this data set (blue) and that measured from the competing RNA solution (chamber C_{III}, in red) are shown. Intensity ratios are indicated. (b) Selectivity profiles derived for libraries **M**−**Q** in experiments 1a−3a (see the main text). Those obtained with the individual libraries are included for comparison (black circles). (c) Affinity profiles (see the main text) measured from the 20 kanamycin derivatives (libraries **M**−**Q**) in experiment 3a. (d) MD ensembles derived for the **B2**/A-site, and **T4**/A-site complexes. Ethyl and uracil moieties are represented in yellow. Putative ligand/RNA contacts established through these fragments are highlighted.

DOI: 10.1021/jacs.6b00328
J. Am. Chem. Soc. 2016, 138, 6463−6474

consequently, they preferentially associate to the target A-Site. This effect is particularly evident for the heaviest derivatives (see Figure S16).

Binding Experiments Using Mixtures of Increased Complexity. Finally, we tested the proposed methodology with more complex mixtures formed by up to 4 regioisomer libraries, plus the reference kanamycin derivative (21 pseudo-trisaccharide derivatives in total). Several microdialysis assays were carried out, employing ligand solutions in the 100, 200, and 400 μM range (herein referred as experiments 1a−3a) and a fixed concentration for the RNA fragments (100 μM).

Interestingly, despite their multicomponent character, HSQC experiments acquired from the resulting NMR samples were still well resolved, allowing a straightforward identification of the characteristic methyl cross-peaks for every single derivative (Figure 5a). These reporter signals were employed to evaluate their relative concentration in the three chambers following the protocol aforementioned.

The obtained results are represented in Figure 5b,c. It can be observed that the "selectivity profile" derived from experiment 1a (21 derivatives, ∼100 μM) shows a reasonable agreement with those previously described for the individual libraries (5 derivatives, ∼100 μM. Also included in Figure 5b for comparison purposes). On the contrary, experiments 2a (200 μM) and 3a (400 μM) reveal a distinct behavior, characterized by a gradual decrease in the apparent selectivity of all ligands, which is particularly evident for derivatives **M1**−**M5** and **O1**−**O5**. For example, when library **M** is tested alone, regioisomer **M1** exhibits a clear preference for the A-Site RNA fragment; however, the observed selectivity is, to a large extent, abolished in the context of the more complex mixtures used in experiments 2a and 3a. This behavior reflects the influence that competition among ligands plays in the output of the experiment, and represents the expected consequence of increasing the total aminoglycoside/receptor ratio; under these competition conditions, only sufficiently strong binders are able to reveal their selectivity for the A-Site receptor (for a more detailed explanation of this effect see Figures S3−S7). Accordingly, libraries **P** and **Q** seem to present an overall larger affinity for the A-Site RNA receptor than libraries **M** and **N**. This point was fully confirmed by the "affinity profile" derived from experiment 3a (see Figure 5c). Similar selectivity/affinity profiles were derived with additional combinations of libraries (**C** + **T** and **B** + **J** + **S**) and are shown in the Supporting Information (Figure S17).

In summary, the methodology described herein can be extended to more complex ligand mixtures providing a semiquantitative description of the RNA-binding properties for every single component. At low ligand/RNA ratios, the distribution of the aminoglycoside derivatives in microdialysis chambers C_I and C_{III} can be employed to reveal their relative selectivities. It should be noted that this requirement implies that the amount of every individual component in solution should decrease for increasingly complex mixtures. However, the enhanced sensitivity of modern high-field NMR spectrometers equipped with cryo-probes allows the accurate detection of $^{13}CH_3$ cross-peaks even at concentrations below 2 μM.

DISCUSSION

We present herein a new combinatorial strategy especially suitable for the optimization of multivalent polyamine scaffolds as DNA/RNA ligands. Our protocol provides a quick and easy access to a large variety of small regioisomer libraries that can be tested for selective recognition employing a microdialysis assay. This has been carefully designed to allow competition between two alternative RNA fragments (one specific and a one nonspecific receptor) for the different library components. Therefore, quantification of the latter in the microdialysis compartments provides a full description of the library binding properties. It should be noted that the deconvolution of the resulting mixtures is a nontrivial task. Indeed, they are formed by low concentrations (usually in the 2−25 μM range) of highly similar pseudo-trisaccharide derivatives, lacking in many occasions any chromophoric function. For this reason, we have set up a novel NMR-based approach that combines simplicity and sensitivity. Our strategy is based on the derivatization of the samples with ^{13}C-labeled formaldehyde to yield the corresponding mixtures of per-*N*-^{13}C-methyl derivatives. This modification renders the libraries detectable by NMR methods even at very low concentrations (<2 μM). In addition, it equips every single component with a chemically differentiated methyl group, which is unique within the mixture and, consequently, can be used as reporter for detection and quantification purposes. Indeed, HSQC spectra show that these functions usually produce well-resolved upfield shifted signals in the carbon dimension due to the γ-substituent effect.

Receptor and ligand-based NMR approaches have been widely used in drug development for the last 20 years.[16] These methodologies rely on the unique ability of NMR spectroscopy to detect and analyze binding processes, being especially adequate for drug screening and optimization of binding affinities. However, they present a more limited scope when it comes to dealing with key aspects of the recognition process like selectivity. Our approach allows for working with multiple ligands and receptors at a time and therefore provides an alternative to existing methods, suitable for affinity/selectivity optimization of complex multivalent leads (a challenging problem in medicinal chemistry). Regarding the analysis and quantification of the ligand mixtures, NMR has shown in recent years great potential in dealing with complex mixtures of compounds.[17] However, in particular cases, NMR capacity to deal with multicomponent chemical systems prior to physical separation can be limited by the lack of appropriate signal dispersion. This feature represents an especially severe problem in cases where all the mixture components present highly similar chemical structures, which is a common situation in the context of a lead optimization process. Of note, our results demonstrate that ^{13}C-labeled libraries formed by highly similar derivatives that share a common scaffold can provide clear spectra in which all the essential information is preserved. The reason for this effect is that extreme overlapping affects mainly those molecular fragments that are common to all library members ($N^{13}Me_2$ in our case), whereas dissimilar regions (such as N^{13}**Me**R) tend to produce well-resolved non-overlapped peaks. Indeed, according to our data, mixtures formed by up to 21 pseudo-trisaccharide derivatives bearing diverse aromatic units at different sites render perfectly tractable HSQC spectra.

Altogether, this experimental data has allowed the identification of several kanamycin derivatives that display improved selectivity and/or affinity for the ribosomal A-site oligo (as derivatives **B2**, **T4** or libraries **P**−**Q**).[18] Molecular modeling efforts based on Molecular Dynamics (MD) simulations (see the Experimental Section and Figure 5d) provide plausible hypotheses for some of these cases. According to them, the

DOI: 10.1021/jacs.6b00328
J. Am. Chem. Soc. 2016, 138, 6463−6474

favorable influence exerted by alkyl chains at position 3-III (as in **B2**), a phenomenon previously reported for methyl and ethyl substitutions and correctly reproduced by our assays,[10,15] might have its origin in the establishment of additional CH/δ contacts between the alkylic chain and the RNA bases (reminiscent of the so-called cation-δ stair motif, Figure 5d).[19] Similarly, additional hydrogen bonding interactions between the uracil fragment and the RNA base pairs could be invoked to rationalize the enhanced binding properties detected for **T4** (Figure 5d). On the contrary, a kanamycin-like binding mode would be clearly unfeasible for other derivatives (such as those present in libraries **P** or **Q**). Although merely speculative, these libraries might exhibit alternative binding modes, perhaps dominated by intercalation of the aromatic fragment between the RNA bases.

Overall, our results demonstrate that there is a significant opportunity to improve the binding properties of polyamine binders and that, in fact, this goal can be achieved by relatively simple chemical modifications.

CONCLUSIONS

We propose a fast, simple and highly parallelizable combinatorial methodology for the optimization of polyamine nucleic acid binders. The pivotal element of our protocol involves the use of a novel isotopic labeling/NMR strategy that combines simplicity and sensitivity, allowing the analysis and quantification of ligand mixtures formed by a low concentration of highly similar pseudo-trisaccharide derivatives. In principle, this approach could be applied to the development of improved ligands for a wide variety of biologically relevant DNA/RNA targets. The extension of this concept to other molecular binders can also be envisaged. Thus, simple polyamine scaffolds amenable for optimization could be designed and synthesized. Alternatively, they could be obtained form natural sources. Certainly, aminoglycosides constitute the most evident choice, providing a significant number of structurally diverse candidates. However, different choices, as those represented by small cationic peptides, could also be considered. In comparison with conventional medicinal chemistry approaches, our protocol provides significantly cheaper and faster avenues to the optimization of nucleic acid binders.

EXPERIMENTAL SECTION

Synthesis of the Reference Kanamycin-B Derivative. A kanamycin-B derivative, equipped with one ^{13}C-labeled OMe group in position 6-III (see Figure 2), was prepared following the procedure previously described for the unlabeled compound.[12]

Library Generation. Tailored Kanamycin-B regioisomer libraries **A**−**T** were prepared through reductive amination reactions. Thus, aminoglycoside solutions (1 mL, 50−70 mM) in phosphate buffer (10 mM) at pH 7.8, were treated with a substoichiometric amount of corresponding aldehyde (5−10 mM) and sodium cyanoborohydride (20 mM). Library **A** was generated in its labeled form, employing ^{13}C-formaldehyde. In contrast, for the generation of cocktails **B**−**T**, we used the unlabeled aldehydes. After 12 h at room temperature, the reaction mixtures were evaporated under vacuum and the resulting residues were purified by flash chromatography. In all cases, a mixture of the five mono-N-substituted kanamycin regioisomers could be separated from a large excess of the unmodified aminoglycoside. Stock solutions in D_2O (1 mL, total aminoglycoside concentration 1−7 mM) were prepared for the different kanamycin libraries. Selected libraries were also generated by performing the reductive amination reaction at alternative pH values in the 4.5−9.5 range. This procedure yielded mixtures with alternative regioisomer distributions.

Kanamycin-B libraries **A**−**T** were characterized by mass spectrometry. In addition, library A and permethylated **B**−**T** samples were also dissected by NMR spectroscopy. To this end, **B**−**T** library solutions in 500 μL of D_2O (total aminoglycoside concentration ∼0.5 mM) were prepared from the different stocks and treated with ^{13}C-formaldehyde (15 mM) and sodium cyanoborohydride (20 mM) at pH 6.0. After 10 h, the pH of the reaction mixtures was adjusted to be >10. Next, samples were transferred to NMR tubes and analyzed by means of HSQC and HMBC experiments. HSQC spectra acquired for library **A** and the 19 generated permethyl kanamycin libraries (**B**−**T**) are shown in Figures S10 and S11. It should be noted that in this latter case, derivatization with formaldehyde equips every library component with a distinct −N^{13}**Me**R methyl group that can be used as reporter for detection and quantification purposes. HSQC spectra show that these functions produce, in all cases, well-resolved signals upfield shifted in the carbon dimension with respect to those of the −N^{13}Me$_2$ groups. In addition, they exhibit clear three-bond connections in HMBC spectra, not only with the kanamycin scaffold but also with the attached chemical fragments (R) (HMBC spectra acquired for selected permethyl libraries are represented in Figure S12).

Preparation of RNA Fragments. RNA fragments, including the 27-mer A-site sequence and the 26-mer mutated variant were obtained employing an in vitro transcription as previously described.[20]

Microdialysis Protocol: Theoretical Simulations. We performed extensive modeling studies on the microdialysis competition experiment described in the manuscript (see Figures S3−S7), employing the biochemical kinetic simulator GEPASI.[21] Our model (Figure S3) comprised a small library formed by five ligands, initially placed in the central chamber of a three-compartment microdialysis device. Two alternative RNA solutions are confined in lateral chambers I and III. Chamber volumes and RNA concentrations were fixed at 400 μL and 100 μM, respectively, in agreement with the actual conditions employed in our experimental assays. Numeric integration of the corresponding kinetic equations allowed a theoretical evaluation of the equilibrium ligand concentrations in chambers C_I−C_{III}, assuming a large variety of scenarios.

Our theoretical treatment demonstrates that the employed selectivity parameter (**Sel**) constitutes a good indicator of the ligand selectivity provided that

(a) Total library concentration does not largely exceed that of the RNA fragments (100 μM in most of our experiments).
(b) Binding affinities (K_b) of the library components to the ribosomal A-site are in the 10^5 M^{-1} range or larger.

According to our data, under these circumstances **Sel** values show a strong linear correlation with the actual selectivity of the library components (defined as the ratio between their affinities for the competing RNA fragments, K_{b1}/K_{b2}). Therefore, most promising compounds, in terms of discriminating capacity, can be easily identified, even in the presence of stronger binders (see Figures S3−S7).

At increasing library concentrations, the concentration of RNA receptor becomes limiting so that the fraction of uncomplexed ligands increases and **Sel** parameters gradually tends to unity (see eq 1 in Figure S3). Interestingly, this effect is more pronounced for weak binders (as experimentally observed for ligand **M1** in the last section of the manuscript. Figure 5c). As a consequence, under these circumstances, the previously observed correlation (between **Sel** and K_{b1}/K_{b2} ratios; see Figures S4−S7) could be significantly reduced. However, these experiments still afford valuable clues about the relative affinity of the mixture components. In our opinion, microdialysis assays performed with different library concentrations provide a more complete picture of the library association properties and represent a source of information for optimization purposes.

Regarding the affinity parameter (denoted as **Af** throughout the manuscript and taken as indicative of the relative binding strength of the different mixture components), the theoretical values showed a perfect correlation with the binding affinities to the A-site (K_{b1}) under all the simulation conditions tested (see Figure S7).

DOI: 10.1021/jacs.6b00328
J. Am. Chem. Soc. 2016, 138, 6463−6474

Microdialysis Protocol: Experimental Details. Lyophilized samples of the RNA fragments were dissolved in 400 μL of buffer (10 mM phosphate, 100 mM NaCl, 1 mM $MgCl_2$ at pH 7.0) to a final concentration of 100 μM, renatured by heating to 85 °C for 1 min and then slowly cooling back to 20 °C over a 2 h period. Similarly, 400 μL of library solutions were prepared from stocks in the same buffer. These also contained the reference $O^{13}CH_3$−Kanamycin-B derivative (**Ref**). The resulting solutions were loaded in the central compartment (herein referred as C_{II}) of a three-chamber microequilibrium dialyzer (Harvard apparatus) equipped with 5 K_d cutoff membranes and dialyzed against the two separate 400 μL of RNA solutions (see Figure 2).

Different RNA and library concentrations were extensively tested. Final experiments were performed employing 100 μM RNA solutions. Similarly, aminoglycoside mixtures were carefully adjusted so that the total concentration of kanamycin regioisomers and that of the reference compound (**Ref**) amounts to 80−130 and 15−25 μM (roughly the average concentration for the single library components), respectively. To achieve a complete equilibration of the three microdialysis compartments, these assays were left to proceed for 3 days at 35 °C. The chemical stability of the RNA fragments and selected libraries throughout the microdialysis experiments was carefully checked. In all cases, no evidence of chemical evolution was found for any of the samples tested.

Control experiments were performed employing the same RNA solution in both microdialysis compartments. In addition, aminoglycoside mixtures containing different population of the single regioisomer derivatives were also tested. Some of these assays are described in Figures 4 and S13.

Sample Derivatization and NMR Data Acquisition. Solutions from the three microdialysis compartments (chambers C_I-C_{III}) were collected and the RNA fragments were digested with ribonuclease-B (1−2 μM) for 12 h. Next, aminoglycoside mixtures (**B**−**T**) present in the three samples were derivatized by treatment with ^{13}C-labeled formaldehyde (30 mM) and sodium cyanoborohydride (40 mM). After 12 h at room temperature, the solutions were lyophilized and resuspended in 500 μL of D_2O, containing 90 μM ^{13}C-labeled sodium acetate as internal reference for concentrations, as previously described.[10] The pH of these samples was adjusted to 10. For library **A**, no derivatization was required prior to the NMR analysis.

HSQC and HMBC spectra were acquired in Bruker Avance 800 MHz and Bruker Avance 600 MHz spectrometers equipped with cryoprobes. For the 800 MHz experiments, a data matrix of 2K*1K was typically used to digitize a spectral width of 4000 Hz in F2 and 15 000 Hz in F1. We used 16 scans per increment with a relaxation delay of 1 s and a delay corresponding to a J value of 145 Hz.

To evaluate the concentration of the different aminoglycoside components in the different samples, key reporter cross-peaks in HSQC experiments were integrated employing Bruker software. We also acquired control HSQC spectra with alternative relaxation delays (in the 1−4 s range) to determine the influence of this parameter on the estimated concentrations (Figure S14).

A selectivity parameter (**Sel**) was defined for every single kanamycin derivative as the ratio between its equilibrium concentrations in chambers C_I and C_{III}. Similarly, in particular cases (see Figures 5 and S17), affinities were estimated from the equilibrium concentrations in chambers C_I and C_{III} (**Af**). Both indicators were divided by those obtained for the Reference compound (**Ref**) present in all the microdialysis assays (normalized **Sel** and **Af** values are denoted as $\mathbf{Sel}_N$ and $\mathbf{Af}_N$ throughout the manuscript). In this way, the binding properties could be compared between different libraries/experiments.

Molecular Dynamics Simulations. The experimental structure of the A-site/gentamycin (pdb code: 2ET3) complex was employed as starting coordinates for molecular dynamic (MD) simulations. After replacing this ligand with the different kanamycin-B derivatives herein considered, MD simulations were carried out, using the sander module within the AMBER 12 package.[22] RESP atomic charges for the aminoglycosides were derived by applying the RESP module of AMBER to the HF/6-31G(d) ESP charges calculated with Gaussian 09.[23] The ffSB14 force field[24] was implemented with GLYCAM06[25] and GAFF[26] parameters to accurately simulate the conformational behavior of these ligands. The 100 ns MD trajectories were collected in the presence of explicit TIP3P water,[27] periodic boundary conditions and Ewald sums for the treatment of long-range electrostatic interactions[28] as previously described.[29] The time step was 2 fs in all the simulations.

Quantum Mechanical Calculations. Cyclohexane monosubstituted with either NMe_2 or NMeR (R = ethyl, benzyl, or cyclopropylmethyl) groups at the equatorial position were considered as abbreviated models for selected kanamycin derivatives. All geometry optimizations were carried out with the Gaussian 09 software[23] using the M06-2X hybrid functional[30] in combination with the TZVP basis set[31] and ultrafine integration grids. The possibility of different conformations was taken into account for all structures. Frequency analyses were carried out at the same level used in the geometry optimizations, and the nature of the stationary points was determined in each case according to the appropriate number of negative eigenvalues of the Hessian matrix. Scaled frequencies were not considered. Bulk solvent effects (i.e., water) were considered implicitly during geometry optimization through the IEFPCM polarizable continuum model.[32] NMR chemical shifts were calculated at the equilibrium geometries for all conformers with the GIAO29-31[33−35] method at the IEFPCM(water) /mPW1PW91/6-311+G(2d,p) level using ultrafine integration grids. The upfield shift ("γ effect") of the conformationally weighted carbon signals of the different −N**Me**R groups was derived using the values for the NMe_2 moiety as a reference.

■ ASSOCIATED CONTENT

Supporting Information

The Supporting Information is available free of charge on the ACS Publications website at DOI: 10.1021/jacs.6b00328.

Brief description of the rationale behind the selection of the library fragments; Figures S1−S20 and Table S1 showing details of the screening protocol and the microdialysis/NMR experiments carried out (PDF)

■ AUTHOR INFORMATION

Corresponding Author

*juanluis.asensio@csic.es

Notes

The authors declare no competing financial interest.

■ ACKNOWLEDGMENTS

This investigation was supported by research grants of the Spanish "Plan Nacional" (MINECO) CTQ2013-45538-P, CTQ2012-32025, and CTQ2012-32114. E.J.-M. and L.M.-J. thank MINECO for contracts BES-2011-044466 and BES-2014-070232, respectively. BiFi is gratefully acknowledged for supercomputer support (Memento cluster). We also thank CESGA (Santiago de Compostela) for computer support.

■ REFERENCES

(1) (a) Talaska, A. E.; Schacht, J. In *Aminoglycoside Antibiotics: From Chemical Biology to Drug Discovery*; Arya, D. P., Ed.; Wiley Series in Drug Discovery and Development; Wiley. 2007. (b) Schroeder, R.; Waldsich, C.; Wank, H. *EMBO J.* **2000**, *19*, 1−9. (c) Walter, F.; Vicens, Q.; Westhof, E. *Curr. Opin. Chem. Biol.* **1999**, *3*, 694−704. (d) Thomas, J. T.; Hergenrother, P. J. *Chem. Rev.* **2008**, *108*, 1171−1224. (e) Sucheck, S. J.; Wong, C. H. *Curr. Opin. Chem. Biol.* **2000**, *4*, 678−686.

(2) (a) Fourmy, D.; Recht, M. I.; Blanchard, A. C.; Puglisi, J. D. *Science* **1996**, *274*, 1367−1371. (b) Mikkelsen, N. E.; Johansson, K.; Virtanen, A.; Kirsebom, L. A. *Nat. Struct. Biol.* **2001**, *8*, 510−514. (c) Jiang, L. C.; Patel, D. J. *Nat. Struct. Biol.* **1998**, *5*, 769−774.

DOI: 10.1021/jacs.6b00328
J. Am. Chem. Soc. 2016, 138, 6463−6474

(d) Jiang, L. C.; Majumdar, A.; Hu, W. D.; Jaishree, T. J.; Xu, W. K.; Patel, D. J. *Structure* **1999**, *7*, 817−827. (e) Ennifar, E.; Paillart, J. C.; Bodlenner, A.; Walter, P.; Weibel, J. M.; Aubertin, A. M.; Pale, P.; Dumas, P.; Marquet, R. *Nucleic Acids Res.* **2006**, *34*, 2328−2339. (f) Lapidot, A.; Vijayabaskar, V.; Litovchick, A.; Yu, J.; James, T. L. *FEBS Lett.* **2004**, *577*, 415−421. (g) Jiang, L.; Suri, A. K.; Fiala, R.; Patel, D. J. *Chem. Biol.* **1997**, *4*, 35−50. (h) Shalev, M.; Kondo, J.; Kopelyanskiy, D.; Jaffe, C. L.; Adir, N.; Baasov, T. *Proc. Natl. Acad. Sci. U. S. A.* **2013**, *110*, 13333−13338. (i) Jia, X.; Zhang, J.; Sun, W.; He, W.; Jiang, H.; Chen, D.; Murchie, A. I. H. *Cell* **2013**, *152*, 68−81.

(3) (a) Francois, B.; Szychowski, J.; Sekhar, S.; Pachamuthu, A. K.; Swayze, E. E.; Griffey, R. H.; Migawa, M. T.; Westhof, E.; Hanessian, S. *Angew. Chem., Int. Ed.* **2004**, *43*, 6735−6738. (b) Blount, K. G.; Zhao, F.; Hermann, T.; Tor, Y. *J. Am. Chem. Soc.* **2005**, *127*, 9818−29. (c) Liang, F. S.; Wang, S. K.; Nakatani, T.; Wong, C. H. *Angew. Chem., Int. Ed.* **2004**, *43*, 6496−6500. (d) Bastida, A.; Hidalgo, A.; Chiara, J. L.; Torrado, M.; Corzana, F.; Cañadillas, J. M.; Groves, P.; Garcia-Junceda, E.; Gonzalez, C.; Jimenez-Barbero, J.; Asensio, J. L. *J. Am. Chem. Soc.* **2006**, *128*, 100−116. (e) Asensio, J. L.; Hidalgo, A.; Bastida, A.; Torrado, M.; Corzana, F.; Junceda, E. J.; Canada, J.; Chiara, J. L.; Jiménez-Barbero, J. *J. Am. Chem. Soc.* **2005**, *127*, 8278−8279. (f) Matsushita, T.; Chen, W.; Juskeviciene, R.; Teo, Y.; Shcherbakov, D.; Vasella, A.; Bottger, E. C.; Crich, D. *J. Am. Chem. Soc.* **2015**, *137*, 7706−7717. (g) Ennifar, E.; Aslam, M. W.; Strasser, P.; Hoffmann, G.; Dumas, P.; van Delft, F. L. *ACS Chem. Biol.* **2013**, *8*, 2509−2517.

(4) (a) Xi, H.; Davis, E.; Ranjan, N.; Xue, L.; Hyde-Volpe, D.; Arya, D. P. *Biochemistry* **2011**, *50*, 9088−9113. (b) Arya, D. P.; Coffe, R. L.; Willis, B.; Abramovitch, A. I. *J. Am. Chem. Soc.* **2001**, *123*, 5385−5395. (c) Arya, D. P.; Xue, L.; Willis, B. *J. Am. Chem. Soc.* **2003**, *125*, 10148−10149. (d) Arya, D. P.; Coffee, R. L.; Charles, I. *J. Am. Chem. Soc.* **2001**, *123*, 11093−11094. (e) Arya, D. P.; Willis, B. *J. Am. Chem. Soc.* **2003**, *125*, 12398−12399.

(5) Wong, C. H.; Hendrix, M.; Priestley, E. S.; Greenberg, W. A. *Chem. Biol.* **1998**, *5*, 397−406.

(6) Ryu, D. H.; Litovchick, A.; Rando, R. R. *Biochemistry* **2002**, *41*, 10499−10506.

(7) (a) Deng, H.; Bloomfield, V. A.; Benavides, J. M.; Thomas, G. J. *Nucleic Acids Res.* **2000**, *28*, 3379−3385. (b) Kabir, A.; Kumar, G. S. *PLoS One* **2013**, *8*, e70510.

(8) (a) Gordon, E. M.; Gallop, M. A.; Patel, D. V. *Acc. Chem. Res.* **1996**, *29*, 144−154. (b) Thompson, L. A.; Ellman, J. A. *Chem. Rev.* **1996**, *96*, 555−600.

(9) (a) Ramstrom, O.; Lehn, J. M. *Nature* **2002**, *1*, 26−36. (b) Corbett, P. T.; Leclaire, J.; Vial, L.; West, K. R.; Wietor, J. L.; Sanders, J. K. M.; Otto, S. *Chem. Rev.* **2006**, *106*, 3652−3711.

(10) Jiménez-Moreno, E.; Gómez-Pinto, I.; Corzana, F.; Santana, A. G.; Revuelta, J.; Bastida, A.; Jiménez-Barbero, J.; González, C.; Asensio, J. L. *Angew. Chem., Int. Ed.* **2013**, *52*, 3148−3151.

(11) Control assays with an alternative RNA receptor are included in the Supporting Information.

(12) Van Schepdael, A.; Delcourt, J.; Mulier, M.; Busson, R.; Verbist, L.; Vanderhaeghe, H. J.; Mingeot-Leclercq, M. P.; Tulkens, P. M.; Claes, P. J. *J. Med. Chem.* **1991**, *34*, 1468−1475.

(13) Grant, D. M.; Paul, E. M. *J. Am. Chem. Soc.* **1964**, *86*, 2984−2990.

(14) (a) Yoshizawa, S.; Fourmy, D.; Puglisi, J. D. *EMBO J.* **1998**, *17* (22), 6437−6448. (b) Lynch, S. R.; Ruben, L.; Gonzalez, Jr.; Puglisi, J. D. *Structure* **2003**, *11*, 43−53. (c) Carter, A. P.; Clemons, W. M.; Brodersen, D. E.; Morgan-Warren, R. J.; Wimberly, B. T.; Ramakrishnan, V. *Nature* **2000**, *407*, 340−348. (d) Vicens, Q.; Westhof, E. *Chem. Biol.* **2002**, *9*, 747−755. (e) Francois, B.; Rusell, R. J. M.; Murray, J. B.; Aboul-ela, F.; Masquida, B.; Vicens, Q.; Westhof, E. *Nucleic Acids Res.* **2005**, *33*, 5677−5690. (f) Kondo, J.; Russell, R. J. M.; Murray, J. B.; Westhof, E. *Biochimie* **2006**, *88*, 1027−1031. (g) Vicens, Q.; Westhof, E. *Structure* **2001**, *9*, 647−658.

(15) Nakagawa, S.; Toda, S.; Abe, Y.; Yamashita, H.; Fujisawa, K.; Naito, T.; Kawaguchi, H. *J. Antibiot.* **1978**, *31*, 675−680.

(16) (a) Barile, E.; Pellecchia, M. *Chem. Rev.* **2014**, *114*, 4749−4763. (b) Lepre, C. A.; Moore, J. M.; Peng, J. W. *Chem. Rev.* **2004**, *104*, 3641−3675. (c) Wu, B.; Barile, E.; De, S. K.; Wei, J.; Purves, A.; Pellecchia, M. *Curr. Top. Med. Chem.* **2015**, *15*, 2032−2042. (d) Bottini, A.; Wu, B.; Barile, E.; De, S. K.; Leone, M.; Pellecchia, M. *ChemMedChem* **2016**, *11*, 919−927.

(17) Novoa-Carballal, R.; Fernandez-Megia, E.; Jiménez, C.; Riguera, R. *Nat. Prod. Rep.* **2011**, *28*, 78−98.

(18) For compounds **Q4** and **T4** this point has been further demonstrated by additional microdialysis assays employing synthetic pure derivatives. See the Supporting Information.

(19) Rooman, M.; Lievin, J.; Buisine, E.; Wintjens, R. *J. Mol. Biol.* **2002**, *319*, 67−76.

(20) (a) Milligan, J. F.; Uhlenbeck, O. C. Synthesis of Small RNAs Using T7 RNA Polymerase. In *Methods iin Enzymology*; Dahlberg, J. E., Abelson, J. N., Eds.; Academic Press: New York, 1989; Vol. *180*, pp 51− 62. (b) Kao, C.; Zheng, M.; Rudisser, S. *RNA* **1999**, *5*, 1268−1272.

(21) (a) Mendes, P. *Comput. Applic. Biosci* **1993**, *9*, 563−571. (b) Mendes, P. *Trends Biochem. Sci.* **1997**, *22*, 361−363.

(22) Case, D. A.; Darden, T. A.; Cheatham, T. E., III; Simmerling, C. L.; Wang, J.; Duke, R. E.; Luo, R.; Walker, R. C.; Zhang, W.; Merz, K. M.; Roberts, B.; Hayik, S.; Roitberg, A.; Seabra, G.; Swails, J.; Götz, A. W.; Kolossváry, I.; Wong, K. F.; Paesani, F.; Vanicek, J.; Wolf, R. M.; Liu, J.; Wu, X.; Brozell, S. R.; Steinbrecher, T.; Gohlke, H.; Cai, Q.; Ye, X.; Wang, J.; Hsieh, M. J.; Cui, G.; Roe, D. R.; Mathews, D. H.; Seetin, M. G.; Salomon-Ferrer, R.; Sagui, C.; Babin, V.; Luchko, T.; Gusarov, S.; Kovalenko, A.; Kollman, P. A. *AMBER 12*; University of California: San Francisco, CA, 2012.

(23) *Gaussian 09*, Revision E.01; Frisch, M. J.; Trucks, G. W.; Schlegel, H. B.; Scuseria, G. E.; Robb, M. A.; Cheeseman, J. R.; Scalmani, G.; Barone, V.; Mennucci, B.; Petersson, G. A.; Nakatsuji, H.; Caricato, M.; Li, X.; Hratchian, H. P.; Izmaylov, A. F.; Bloino, J.; Zheng, G.; Sonnenberg, J. L.; Hada, M.; Ehara, M.; Toyota, K.; Fukuda, R.; Hasegawa, J.; Ishida, M.; Nakajima, T.; Honda, Y.; Kitao, O.; Nakai, H.; Vreven, T.; Montgomery, J. A., Jr.; Peralta, J. E.; Ogliaro, F.; Bearpark, M.; Heyd, J. J.; Brothers, E.; Kudin, K. N.; Staroverov, V. N.; Kobayashi, R.; Normand, J.; Raghavachari, K.; Rendell, A.; Burant, J. C.; Iyengar, S. S.; Tomasi, J.; Cossi, M.; Rega, N.; Millam, J. M.; Klene, M.; Knox, J. E.; Cross, J. B.; Bakken, V.; Adamo, C.; Jaramillo, J.; Gomperts, R.; Stratmann, R. E.; Yazyev, O.; Austin, A. J.; Cammi, R.; Pomelli, C.; Ochterski, J. W.; Martin, R. L.; Morokuma, K.; Zakrzewski, V. G.; Voth, G. A.; Salvador, P.; Dannenberg, J. J.; Dapprich, S.; Daniels, A. D.; Farkas, Ö.; Foresman, J. B.; Ortiz, J. V.; Cioslowski, J.; Fox, D. J. Gaussian, Inc.: Wallingford, CT, 2009.

(24) Hornak, V.; Abel, R.; Okur, A.; Strockbine, B.; Roitberg, A.; Simmerling, C. *Proteins: Struct., Funct., Genet.* **2006**, *65*, 712.

(25) Kirschner, K. N.; Yongye, A. B.; Tschampel, S. M.; González-Outeiriño, J.; Daniels, C. R.; Foley, B. L.; Woods, R. J. *J. Comput. Chem.* **2008**, *29*, 622.

(26) Wang, J.; Wolf, R. M.; Caldwell, J. W.; Kollman, P. A.; Case, D. A. *J. Comput. Chem.* **2004**, *25*, 1157.

(27) Jorgensen, W. L.; Chandrasekhar, J.; Madura, J. D.; Impey, R. W.; Klein, M. L. *J. Chem. Phys.* **1983**, *79*, 926.

(28) Darden, T.; York, D.; Pedersen, L. *J. Chem. Phys.* **1993**, *98*, 10089.

(29) Madariaga, D.; Martínez-Sáez, N.; Somovilla, V. J.; García-García, L.; Berbis, M. A.; Valero-Gónzalez, J.; Martín-Santamaría, S.; Hurtado-Guerrero, R.; Asensio, J. L.; Jiménez-Barbero, J.; Avenoza, A.; Busto, J. H.; Corzana, F.; Peregrina, J. M. *Chem. - Eur. J.* **2014**, *20*, 12616.

(30) Zhao, Y.; Truhlar, D. *Theor. Chem. Acc.* **2008**, *120*, 215.

(31) Weigend, F.; Ahlrichs, R. *Phys. Chem. Chem. Phys.* **2005**, *7*, 3297.

(32) Scalmani, G.; Frisch, M. J. *J. Chem. Phys.* **2010**, *132*, 114110.

(33) London, F. J. *J. Phys. Radium* **1937**, *8*, 397.

(34) Wolinski, K.; Hinton, J. F.; Pulay, P. *J. Am. Chem. Soc.* **1990**, *112*, 8251.

DOI: 10.1021/jacs.6b00328
J. Am. Chem. Soc. 2016, 138, 6463−6474

(35) Cheeseman, J. R.; Trucks, G. W.; Keith, T. A.; Frisch, M. J. *J. Chem. Phys.* **1996**, *104*, 5497.

DOI: 10.1021/jacs.6b00328
J. Am. Chem. Soc. 2016, 138, 6463−6474